frontiers | Frontiers in Materials

TYPE Original Research
PUBLISHED 05 April 2024
DOI 10.3389/fmats.2024.1378089

Check for updates

OPEN ACCESS

EDITED BY
Zhigang Zhang,
Chongqing University, China

REVIEWED BY
Hui Li,
Hebei University of Technology, China
Mingfeng Xu,
State Key Laboratory of Building Safety and Environment, China

*CORRESPONDENCE
Jin Hou,
houjin1976@hotmail.com

RECEIVED 29 January 2024
ACCEPTED 18 March 2024
PUBLISHED 05 April 2024

CITATION
Hou J, Bai J, Mou H and Xiang Z (2024), Tensile properties and constitutive model of cost-effective multiscale hybrid fiber reinforced strain hardening cementitious composites.
Front. Mater. 11:1378089.
doi: 10.3389/fmats.2024.1378089

COPYRIGHT
© 2024 Hou, Bai, Mou and Xiang. This is an open-access article distributed under the terms of the Creative Commons Attribution License (CC BY). The use, distribution or reproduction in other forums is permitted, provided the original author(s) and the copyright owner(s) are credited and that the original publication in this journal is cited, in accordance with accepted academic practice. No use, distribution or reproduction is permitted which does not comply with these terms.

Tensile properties and constitutive model of cost-effective multiscale hybrid fiber reinforced strain hardening cementitious composites

Jin Hou*, Jianjun Bai, Hongmei Mou and Zhisuo Xiang

Zhenjiang Port Group Co., Ltd., Zhenjiang, Jiangsu, China

To enhance the mechanical properties and cost-effectiveness of conventional polyvinyl alcohol fiber reinforced strain hardening cementitious composite (PVA-SHCC), a modified version called multiscale hybrid fiber reinforced SHCC (MsHySHCC) was developed. This new composite incorporates a combination of steel fiber, PVA fiber and calcium carbonate ($CaCO_3$) whisker. Uniaxial direct tensile behaviors (stress-strain relationship, tensile strength, tensile deformation capacity and tensile toughness) of designed MsHySHCCs were investigated and evaluated. The results show that the PVA fibers dominate the ductile behavior and the steel fibers and $CaCO_3$ whiskers effectively affect the strength of MsHySHCCs. The PVA fibers can be partially replaced by $CaCO_3$ whisker and steel fiber, along with an increase in tensile strength and ductility of designed composites. The findings suggest that the configuration of MsHySHCC proves to be a viable approach in simultaneously enhancing the strength and ductility of PVA-SHCC. A semi-theoretical prediction model for tensile constitutive relationship was derived. The comparison of the theoretical results with the experimental data shows that this semi-theoretical model is applicable for determining the tensile constitutive relationship of PVA-SHCCs and MsHySHCCs.

KEYWORDS

strain hardening cementitious composite, tensile behavior, hybrid fiber, calcium carbonate whisker, constitutive relationship

1 Introduction

Strain hardening cementitious composite (SHCC) is a kind of cementitious composite with high ductility (Liu et al., 2020; Arain et al., 2023). In SHCC preparation, PVA fiber and PE fiber are commonly utilized (Zhang et al., 2021; Zhang et al., 2023a; Khalil and Atta, 2023; Tran and Nguyen, 2023). Out of all these, PVA-SHCC stands as the extensively researched and utilized fiber reinforced material. Nevertheless, the high expense remains a significant obstacle for PVA-SHCC to be implemented in extensive engineering projects (Zhang et al., 2020).

Hybrid use of low cost fibers is one of the effective ways to decrease the material cost of PVA-SHCC (Maalej et al., 2012; Liu et al., 2020; Rawat et al., 2022; Qasim et al., 2023), especially for the hybridization of PVA fiber and micro steel fiber (SF/PVA-SHCC). A lot of previous literatures have reported the tensile performance of SF/PVA-SHCCs. Ramasamy

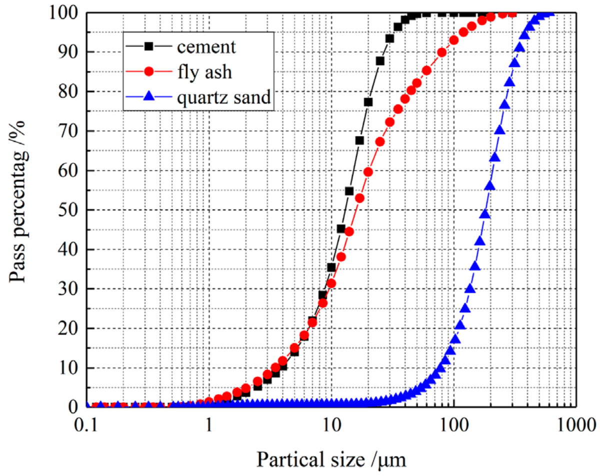

FIGURE 1
Particle size distribution curves of raw materials.

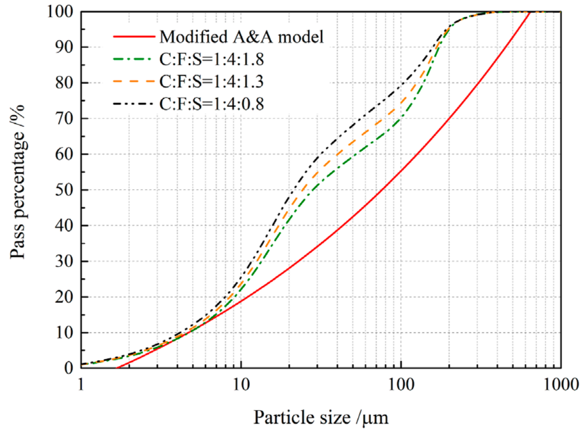

FIGURE 2
Calculation curves based on modified A&A model (C, cement; F, fly ash; S, sand).

and Shanmughasundaram, (2018) reported the mechanical properties of SF/PVA-SHCC containing 0.65% PVA fibers and 1.35% steel fibers. The experimental tensile strength and ultimate tensile strain are 6.78 MPa and 0.98%, respectively. Ramasamy's research found that the steel fiber content exceeded that of PVA fiber, resulting in a comparatively elevated tensile strength but relatively limited tensile ductility. Similar results were also noted in other studies (Hermes et al., 2012; Feng, 2019). It seems that the tensile ductility of SF/PVA-SHCC isn't mainly dominated by steel fibers. Wang et al. (2014) studied the tensile behavior of SF/PVA-SHCCs made by 0.3% steel+1.7% PVA fibers and 0.6% steel+1.7% PVA fibers. The tensile strength of these two kinds of SF/PVA-SHCCs is 3.72 and 4.02 MPa, respectively, while the ultimate tensile strain is 2.39% and 1.97%, respectively. It seems that the combination of high content of PVA fiber and low content of steel fiber can obtain a relatively high tensile ductility, but can't achieve a relatively high tensile strength. Similar experimental results were also pointed out by Liu and Tan. (2017a); Pourfalah (2018); Zhao et al. (2020); Tinoco and Silva (2021).

However, the influence of the content of steel fiber and PVA fiber on the tensile behaviors of SHCC is not completely consistent with the change laws discussed above. A lot of studies have attempted to achieve both high tensile strength and ductility via further adjusting fiber content, introducing highly reactive mineral admixtures, lowing water-binder ratio and optimizing the sand-binder ratio (Zhang et al., 2016; Liu et al., 2017b; Deshpande et al., 2019). However, it is regrettable that we are still far from this idea. Despite the high concentration of steel fibers and PVA fibers in certain research studies, the obtained experimental outcomes remain dissatisfactory (Zhang et al., 2016; Deshpande et al., 2019). As has been reported in Zhang's study, the combination of 1% steel fiber and 2% PVA fiber obtained a very high tensile strength (7.22 MPa), while the ultimate tensile strain was relatively low (0.8%) (Zhang et al., 2016). Therefore, it still needs to find an effective way to optimize the tensile strength and ductility of SF/PVA-SHCC.

It is widely recognized that cementitious materials possess distinct structural characteristics at multiple levels, including the levels of cement hydration products, cement paste, mortar, and concrete (Koichi et al., 2003; Kang and Bolander, 2016). Theoretically, the performance of cementitious materials can be significantly improved by incorporating multi-scale hybrid fibers, spanning from the microscopic to the macroscopic level (Parant and Rossi, 2007a; Parant and Rossi, 2007b; Pierre and Edouard, 2008; Rossi and Parant, 2008; Zhang and Cao, 2014; Cao et al., 2015). However, it is clear that achieving this task solely with steel fiber and PVA fiber is challenging. According to reports, it is believed that the size of fibers, particularly their diameter, has an inverse relationship with their ability to delay the development of microscopic cracks (Betterman et al., 1995; Cao et al., 2013). The dimensions of commonly used PVA fiber and steel fiber do not align well with the microscopic scale of cement hydration product and microscopic cracks, consequently failing to effectively improve the microscopic characteristics of cementitious materials. Hence, it is imperative to discover a viable approach to further augment the microscopic properties of SF/PVA-SHCC.

In recent times, SHCC's mechanical properties were improved using calcium carbonate ($CaCO_3$) whiskers with dimensions of about 30 μm in length and 1 um in diameter. Meanwhile, the cost of $CaCO_3$ whiskers is only about 230 $/t. The enhancement is achieved through microscopic mechanisms such as whisker pull-out, bridging, and crack deflection (Ma et al., 2017; Pan et al., 2018; Cao et al., 2019; Xie et al., 2020). As a result, a composite material named MsHySHCC, which consists of multiple scales of hybrid fibers and exhibits strain hardening properties, was developed. There are two main kinds of MsHySHCC now. The initial type of MsHySHCC solely comprises of PVA fiber and $CaCO_3$ whisker, whereas the second type of MsHySHCC is created by simultaneously incorporating two macro fibers (steel fiber and PVA fiber) and one microscopic fiber ($CaCO_3$ whisker). Mechanical performance and reinforcing mechanism of these two kinds of MsHySHCC have been widely studied. Ma et al. (2017) tested the tensile properties of the aforementioned first kind of MsHySHCC. The experimental findings indicated that $CaCO_3$ whisker increased the tensile strain capacity of PVA-SHCC. However, the strength of the MsHySHCC is comparatively weak, with a compressive

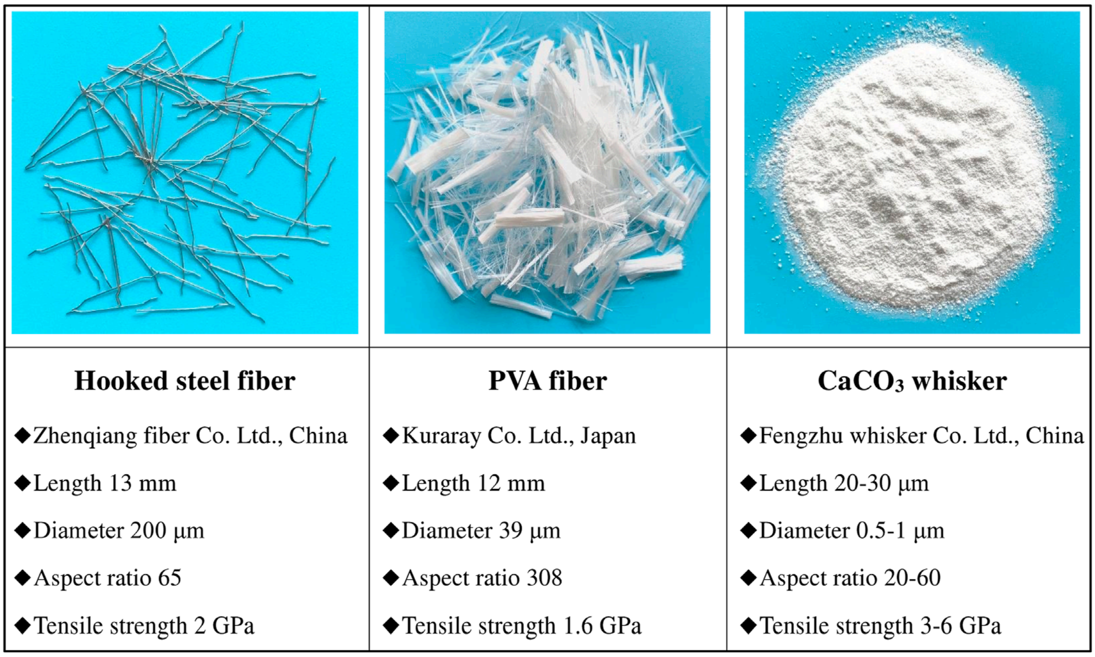

FIGURE 3
Whisker, steel fiber and PVA fiber employed in this paper.

TABLE 1 Fiber content in each designed groups.

Groups	Specification	Steel fiber (SF)/Vol.%	PVA fiber (PVA)/Vol.%	$CaCO_3$ whisker (CW)/Vol.%	Compressive strength/MPa
Control-1	Matrix	0	0	0	39.6
Control-2	CW1	0	0	1	42.8
Control-3	CW2	0	0	2	44.1
PVA-SHCC	PVA2	0	2	0	36.6
MsHySHCC-1	SF0.25PVA1.75CW1	0.25	1.75	1	38.8
MsHySHCC-2	SF0.5PVA1.5CW1	0.5	1.5	1	40.5
MsHySHCC-3	SF0.75PVA1.25CW1	0.75	1.25	1	41.3
MsHySHCC-4	SF0.25PVA1.5CW2	0.25	1.5	2	40.8
MsHySHCC-5	SF0.5PVA1.25CW2	0.5	1.25	2	42.2
MsHySHCC-6	SF0.75PVA1CW2	0.75	1	2	43.7

strength of about 25 MPa and a tensile strength of about 3 MPa. Consequently, this aspect hinders the practical implementation of the designed MsHySHCC. Mechanical properties of PVA-SHCC, which was modified by $CaCO_3$ whiskers (the aforementioned initial type of MsHySHCC), were also documented in Pan's study. It was discovered that the $CaCO_3$ whiskers can be used as a partial replacement for the PVA fibers, resulting in further improvement of the tensile and flexural characteristics of the designed MsHySHCC. However, the concentration of $CaCO_3$ whisker in their research is exceedingly high, consequently elevating the likelihood of whisker agglomeration (Cao et al., 2013). Cao et al. (2019) and Xie et al. (2020) studied the rheological behaviors, mechanical properties and shrinkage performances of MsHySHCC containing steel fiber, PVA fiber and $CaCO_3$ whisker (the aforementioned second kind of MsHySHCC). The researchers discovered that the engineered MsHySHCCs improved the abiligy of the mortar matrix against cracking at multiple scales. However, despite their initial intention to create the SHCC substance through the incorporation of

FIGURE 4
Preparation steps for MsHySHCC.

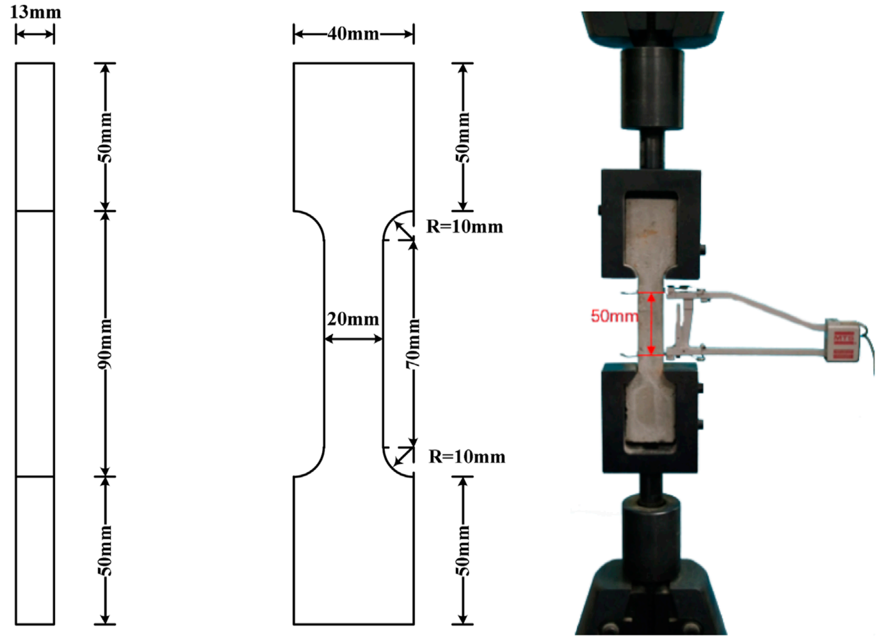

FIGURE 5
Dimension of tensile specimen and tensile test set-ups.

fibers at various scales, the strain hardening characteristics of the developed MsHySHCCs did not meet expectations. Due to the improper consideration of the steel fiber's role in controlling the hardening performance of cementitious materials in their study, the content of steel fiber is higher than that of PVA fiber, resulting in the inability to achieve a high ductility for MsHySHCCs.

From the above previous literatures, it can be noticed that although previous studies focused on MsHySHCC have obtained some relatively rich achievements, there are three basic questions still need to be well responded. (a) What methods can be used to simultaneously enhance the strength and ductility of existing MsHySHCCs? (b) Most of the literatures are experimental studies focus on mechanical properties of MsHySHCC, it still lacking an

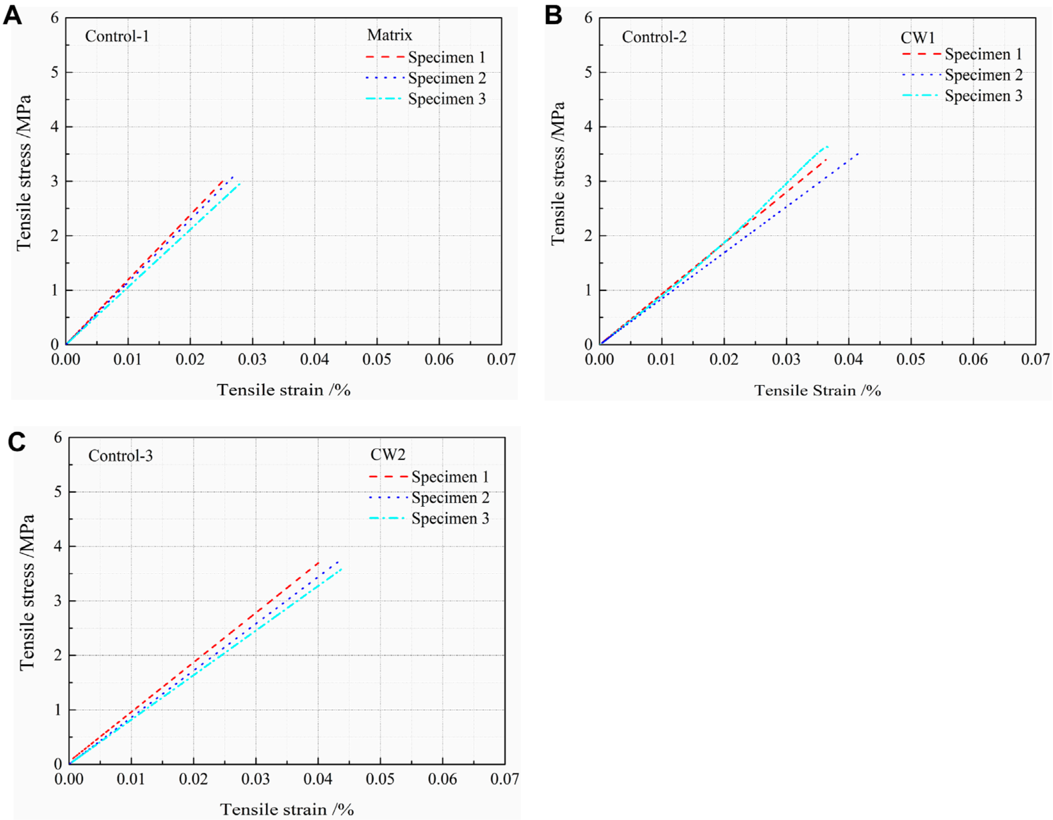

FIGURE 6
Tensile stress-strain relationships of **(A)** matrix; **(B)** 1% $CaCO_3$ whisker and **(C)** 2% $CaCO_3$ whiskers.

TABLE 2 Average values of tensile parameters for control groups.

Groups	Tensile strength/MPa	Ultimate strain/%	Tensile toughness/(N·mm/mm^3)
Control-1	3.027	0.027	0.041
Control-2	3.509	0.038	0.067
Control-3	3.751	0.042	0.079

effective constitutive model to describe the tensile behavior of MsHySHCC, although some micromechanical models and fractural models have been proposed for single fiber type SHCC. To this question, the main difficulties are how to consider the effect of hybrid fibers and most importantly how to take the action of $CaCO_3$ whisker into consideration.

In order to answer the above questions, the following two main works were carried out in this paper. By reasonably adjusting the ratio of matrix, steel fiber, PVA fiber, and $CaCO_3$ whisker, a novel form of MsHySHCC was achieved. Direct tensile performance of this kind of MsHySHCC was characterized, and the balance of strength and ductility of the designed composites was verified. By considering the impact of hybrid fibers and $CaCO_3$ whisker, a semi-theoretical prediction model was given to describe the tensile constitutive relationship of the designed MsHySHCC.

2 Material and experiment

2.1 Raw materials and mix proportion

The components utilized in the matrix included P✓O 42.5 cement, fly ash, and fine quartz sand with a particle size ranging from 100 to 210 μm and an average size of 150 μm. Figure 1 displays the particle size distribution curves for fly ash, sand and cement. The particle size of fly ash is finer compared to cement. It can be used to make the particles of the raw material pack more closely, meanwhile, it has higher hydration activity than low grade fly ash, thus improving the strength of the composite material to a certain extent. Referred to the previous research results (Ma et al., 2017; Zhang et ak., 2020a), the mass ratio of fly ash and cement was set as 4:1 to guarantee a substantial ductility for the designed composite material.

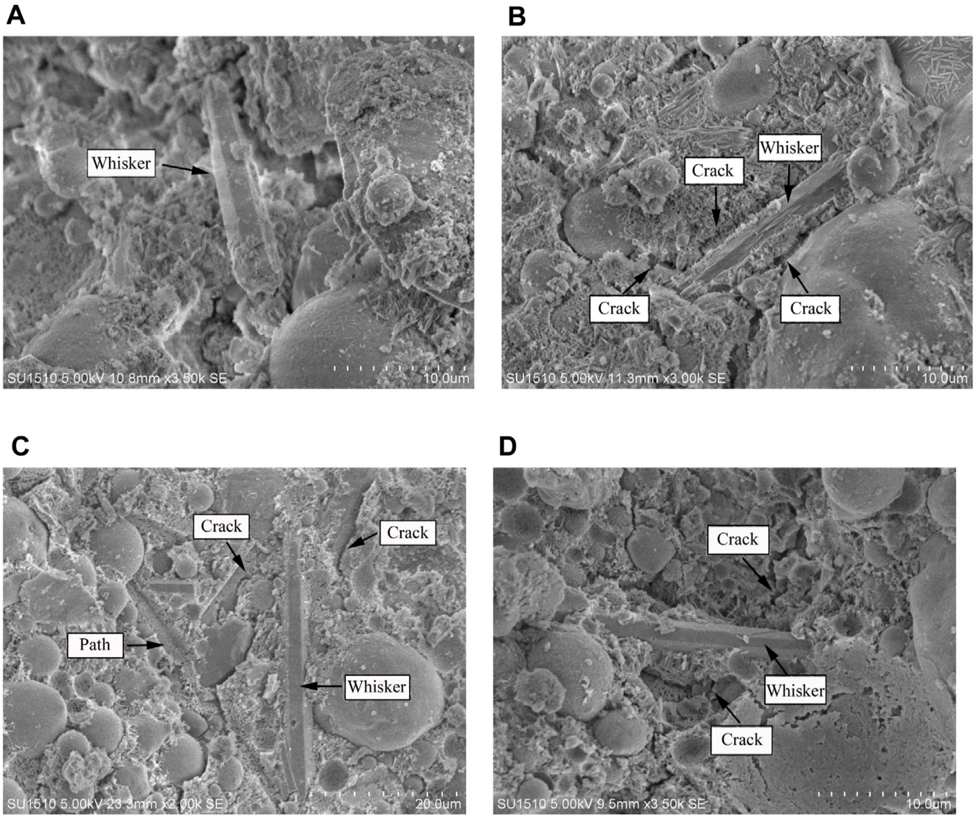

FIGURE 7
Micro-mechanisms of calcium carbonate whisker **(A)** pull-out; **(B)** crack deflection; **(C)** crack deflection and **(D)** bridging.

Previous literatures suggested that the optimal proportion of cement to fine sand should be between 0.6 and 1.8 (Liu and Tan, 2017a; Liu et al., 2017; Ramasamy and Shanmughasundaram, 2018; Tinoco and Silva, 2021; Arain et al., 2023). This study set the mass ratio of sand and cement as 1.8:1 in order to increase the density of the particles, bringing them closer to the theoretical curve, as depicted in Figure 2. More details about the modified A&A model can be obtained in previous literatures (Andreasen and Andersen, 1930; Funk and Dinger, 1994; Hunger, 2010; Karim et al., 2019).

The water to binder ratio was set as 0.34. The fresh MsHySHCC's workability was modified using superplasticizer at 0.5 wt% of binder. Three kinds of reinforcing fibrous materials were employed in this study, as shown in Figure 3. Table 1 displays the composition of various fibers in each designed group. Meanwhile, the 28 days compressive strength (70.7 mm^3 cube) of each group is also give in Table 1. It can be seen that the designed composites had a relative high compressive strength.

2.2 Specimen preparation and testing method

The process of preparing the specimen is illustrated in Figure 4. Dog-bone-shaped specimen was prepared. The tension specimen size is shown in Figures 4, 5. To ensure the precision of the experimental findings, three samples were prepared for every design mixture.

Tensile test set-ups are shown in Figure 5. A 15 mm range extensometer was used to monitor the tensile deformation of the specimen. The tensile loading rate is 0.1 mm/min.

3 Results and discussion

3.1 Tensile stress-strain relationships

Figure 6 shows the tensile stress-strain relationships of control groups with or without $CaCO_3$ whiskers. Table 2 summarizes the average tensile values of strength, ultimate strain and toughness of the three groups of materials. This paper quantifies the tensile toughness by calculating the enclosed region beneath the tensile stress-strain graph, which is employed to assess the specimen's ability to absorb energy under tensile force. By observing Figure 6; Table 2, it becomes evident that $CaCO_3$ whiskers can enhance both the tensile strength and tensile strain capacity of the mortar matrix. And the tensile strength and ultimate strain are further improved with increasing the content of $CaCO_3$ whiskers from 1% to 2%. The enhancements can be explained by the micro-mechanisms of $CaCO_3$ whiskers as illustrated in Figure 7. However, it is worth mentioning that despite the enhancement of tensile properties in the mortar matrix due to the utilization of $CaCO_3$ whisker, the

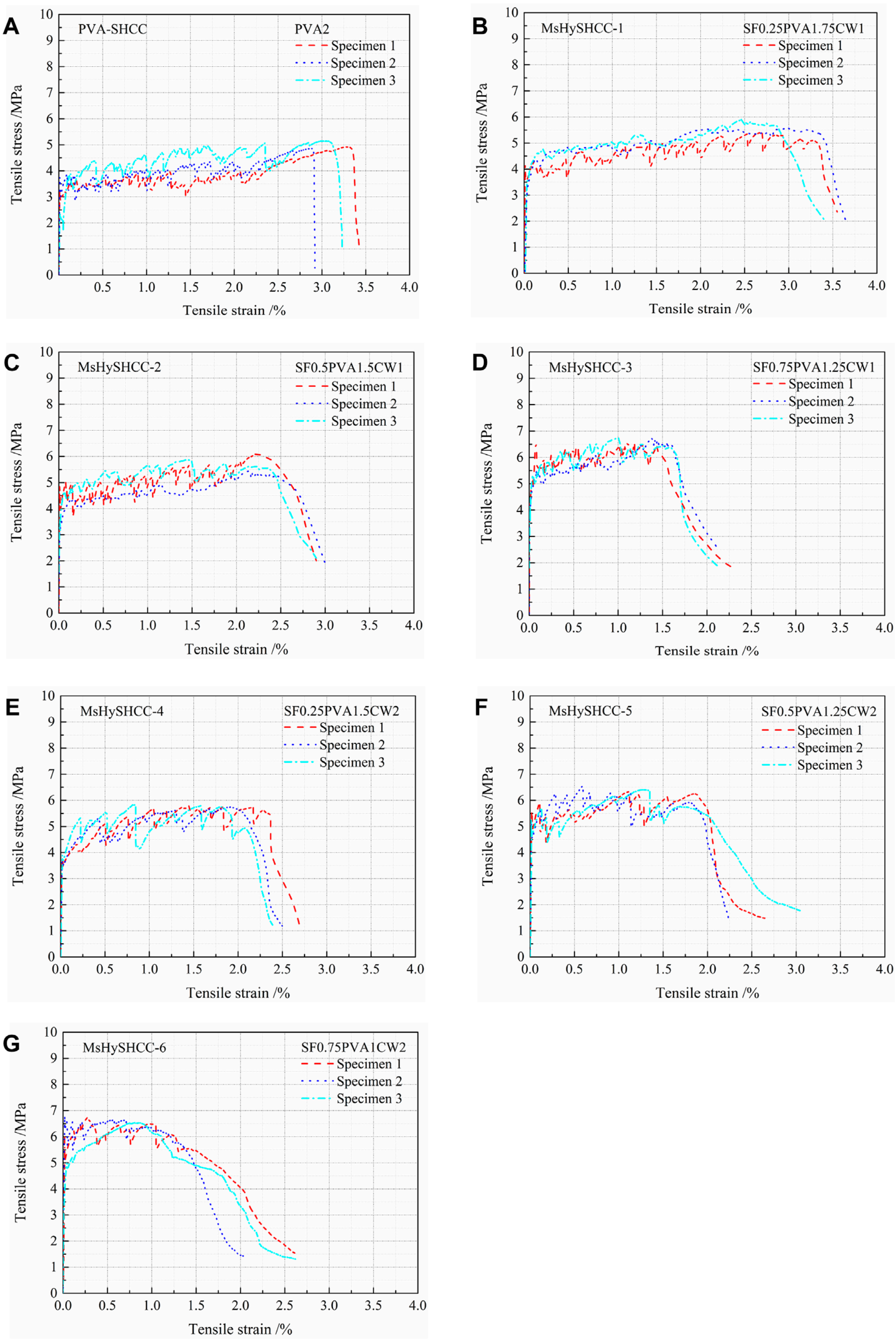

FIGURE 8
Tensile stress-strain relationship curves of MsHySHCCs and PVA-SHCC.

failure process still exhibited evident brittleness and lacked post peak toughness (Cao et al., 2013; Cao et al., 2019). Because the particle size of $CaCO_3$ whisker is small, it can only strengthen and toughen the mortar matrix at the microscopic level, thus can't improve the post peak toughness of the matrix like other macro fibers.

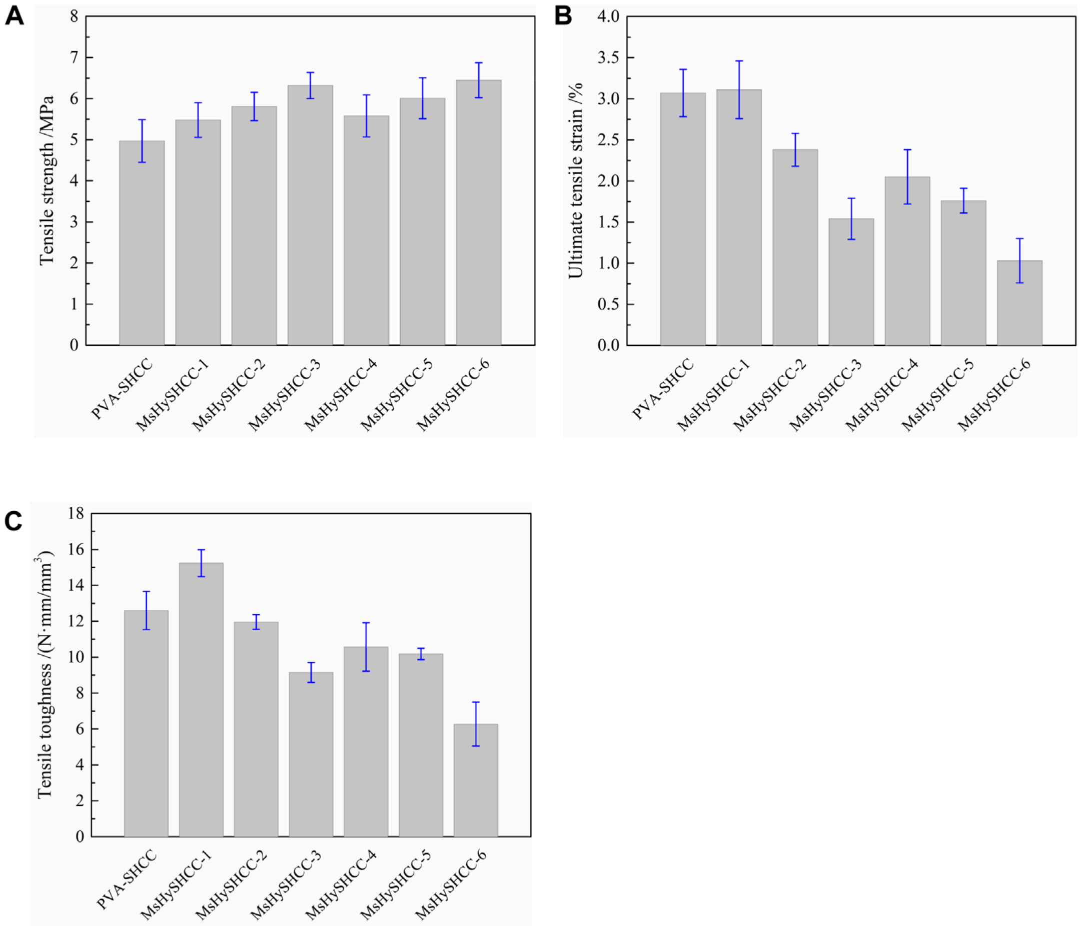

FIGURE 9
Experimental tensile results of **(A)** strength; **(B)** ultimate strain and **(C)** toughness for PVA-SHCC and MsHySHCCs.

The relationship between tensile stress and strain is depicted in Figure 8. Experimental tensile results of strength, ultimate strain and toughness for each group are provided in Figure 9. Experimental data of tensile parameters in previous available literatures are summarized in Table 3. Figure 10 illustrates the comparisons of the experimental findings between previous literature and the current study. From Figures 8–10; Table 3, the following findings can be addressed.

The experimental curves exhibited a slight improvement in robustness when PVA fibers were partially replaced with $CaCO_3$ whiskers and micro hooked steel fibers, as depicted in Figures 8A–G. The microscopic mechanisms of $CaCO_3$ whisker shown in Figure 7 have the potential to enhance the quantity and evenness of micro-cracks within the mortar matrix (Cao et al., 2015; Ma et al., 2017; Pan et al., 2018). Ma et al. (2017) discovered that additional crack sources could potentially contribute to the multiple cracking performance of SHCC (Pan et al., 2018). As a result, it is possible to improve the robustness of the tensile stress-strain curves.

The addition of steel fibers and $CaCO_3$ whiskers to replace some PVA fibers increased the tensile strength of PVA-SHCC. Compared to PVA-SHCC, when the whisker content maintained at 1%, the tensile strength exhibited an increase from 5.48 MPa to 6.32 MPa with the steel fiber content ranging from 0.25% to 0.75%. Increasing the amount of whiskers further enhanced the tensile strength to a small extent, despite the further reduction in PVA fiber content. The enhancements could be credited to the higher peak stress for crack bridging offered by steel fibers with hooks and the reinforcing effect at a microscopic level provided by $CaCO_3$ whiskers. The whiskers and steel fibers have greater modulus of elasticity and stiffness compared to PVA fibers. By limiting the development of cracks, these rigid fibers can effectively improve the principal tensile stress of the material, thus increasing its tensile strength (Rawat et al., 2022; Qasim et al., 2023). On the contrary, PVA fiber is a kind of flexible synthetic fiber that has a lesser impact on the tensile strength compared to steel fiber and $CaCO_3$ whisker.

As depicted in Figure 8; Table 3, MsHySHCC-1 exhibited greater tensile strength and ultimate tensile strain in comparison to PVA-SHCC, with 1% $CaCO_3$ whiskers hybrid 0.25% steel fibers partially replacing 0.25% PVA fibers. Nevertheless, a gradual deterioration in strain hardening behavior of SHCCs was observed when the PVA fiber content was reduced while the steel fiber and $CaCO_3$ whisker amounts were increased. It implies the strain hardening behavior dominates by the PVA fibers. The discrepancy in total quantity between PVA fiber and hooked steel fiber arises due to the constant

TABLE 3 Summary of tensile properties in available literatures and in present study.

Researcher	V_f/%			σ_{tu}/MPa	ε_{tu}/%	Other descriptions
	SF	PVA	CW			
Hermes (2012)	0.75	1.25	—	4.16	0.81	C:FA:S:W = 1:1.2:0.8:0.56
Soe et al. (2013)	0.5	1.5	—	4.73	0.34	C:FA:S:W = 1:1.2:0.8:0.56
	0.58	1.75	—	5.60	0.52	
Wang et al. (2014)	0.3	1.7	—	3.72	2.39	C:S:W = 1:0.3:0.35
	0.6	1.7	—	4.02	1.97	
Tinoco and Silva. (2021)	0.5	1.5	—	4.59	1.88	C:FA:S:W = 1:1.23:1.06:0.665
	1	1	—	4.82	1.79	
Liu and Tan. (2017a)	0.5	1.5	—	5.50	0.8	C:FA:S:W = 1:1.22:1:0.62
Liu et al. (2017b)	0.5	1.5	—	5.48	0.63	C:FA:S:W = 1:1.22:1:0.62
	0.5	1.5	—	4.25	2.08	C:FA:S:W = 1:1.86:0.72:1.03
Zhang et al. (2016)	1	2	—	7.22	0.8	B:S:W = 1:0.833:0.18
Pourfalah (2018)	0.75	1.75	—	4.36	3.0	C:FA:S:W = 1:1.81:0.6:0.78 and l_{sf} = 6 mm
	0.75	1.75	—	4.71	2.5	C:FA:S:W = 1:1.81:0.6:0.78 and l_{sf} = 12 mm
Pan et al. (2018)	—	1.5	2	3.92	2.8	B:S:W = 1:0.2:0.28
	—	1.25	2	3.41	3.22	
	—	1.5	4	3.02	1.97	
	—	1.5	4	3.75	2.15	
Ramasamy and Shanmughasundaram. (2018)	1	1	—	6.30	1.08	C:FA:S:W = 1:0.43:0.71:0.5
	1.35	0.65	—	6.78	0.98	
Liu et al. (2018)	1	1.5	—	5.25	0.65	C:FA:S:W = 1:3:1.4:1.28
Deshpande et al. (2019)	1	2	—	5.85	1.51	C:FA:S:W = 1:2.2:1.3:1.06
Ma et al. (2017)	—	2	0.5	3.29	6.3	C:FA:S:W = 1:4:1.8:1.5
	—	2	1	2.34	6.76	
	—	2	2	2.15	6.77	
	—	5	0.5	2.95	3.43	C:FA:S:W = 1:2.2:1.2:0.96
Zhao et al. (2020)	0.5	2.2	—	3.75	2.95	B:S:W = 1:0.28:0.31
	1	2.2	—	4.71	1.48	
	1.5	2.2	—	4.57	0.82	
Feng (2019)	1.25	0.75	—	5.8	0.13	B:S:W = 1:0.5:0.3
	1.25	0.55	2	5.85	0.16	

(Continued on the following page)

TABLE 3 (*Continued*) Summary of tensile properties in available literatures and in present study.

Researcher	V_f/%			σ_{tu}/MPa	ε_{tu}/%	Other descriptions
	SF	PVA	CW			
Present study	0.25	1.75	1	5.48	3.11	B:S:W = 1:0.36:0.34
	0.5	1.5	1	5.81	2.38	
	0.75	1.25	1	6.32	1.54	
	0.25	1.5	2	5.58	2.05	
	0.5	1.25	2	6.01	1.76	
	0.75	1	2	6.45	1.03	

Note: V_f is the volume fraction of fiber; σ_{tu} is the tensile strength; ε_{tu} is the ultimate tensile strain; l_{sf} is the length of steel fiber; C, cement; FA, fly ash; S, sand; W, water; B, binder.

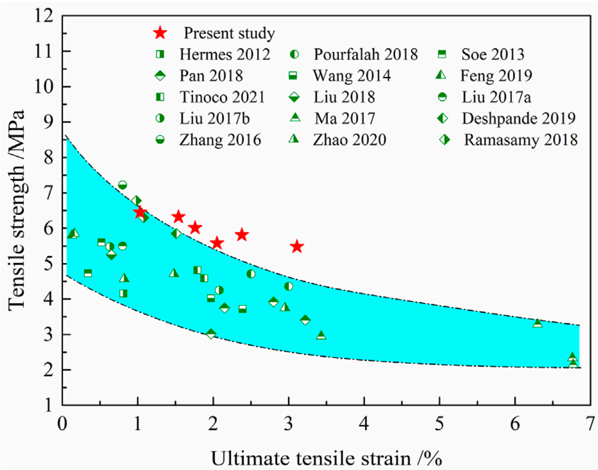

FIGURE 10
Tensile parameters in previous literatures and present study.

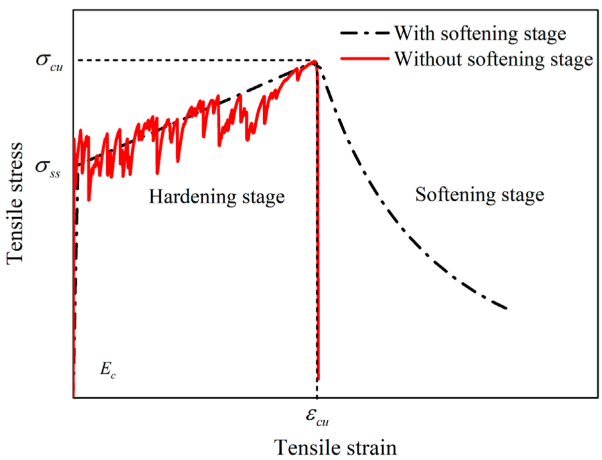

FIGURE 11
Double-line model and triple-line model for SHCC with or without softening stage.

volume content condition. The main determinant for enhancing hardening performance primarily relies on the quantity of fibers rather than just the fiber content. A decrease in the number of fiber pieces results in a reduction in the effective stress caused by fibers, consequently resulting in an unsaturated cracking performance and an unstable hardening process. Meanwhile, although the number of whiskers is very high, the size of the whiskers is tens of times smaller than that of the PVA fibers, so the whiskers can only have a positive effect on microscopic cracks in the matrix. Consequently, the SHCCs don't exhibit significant ductility due to the excessive replacement of PVA fibers with whiskers and hooked steel fibers.

As shown in Table 3; Figure 10, based on the findings, it can be inferred that incorporating PVA fiber, steel fiber, and $CaCO_3$ whisker in the design process of multi-scale fibers is a viable approach to simultaneously enhance the strength and ductility in SHCC.

3.2 Semi-theoretical prediction model

Available literatures have confirmed that double-line model can be used to describe the tensile constitutive relationship of PVA-SHCC, as illustrated in Figure 11. To the SHCC reinforced by steel and PVA hybrid fibers, it may have obvious post-peak softening stage due to the introduction of hooked steel fibers. Generally, the parameter of fiber reinforcing factor RI_v dominates the softening behavior. Previous literatures (Ramasamy and Shanmughasundaram, 2018; Tinoco and Silva, 2021; Deshpande et al., 2019.) show that the softening stage should be considered when $RI_v \geq 1$, which is presented as a triple-line constitutive model, as illustrated in Figure 11. However, through the experimental results in this paper, it is found that when $CaCO_3$ whiskers are added, a relatively obvious softening behavior begins to appear when $RI_v \geq 0.876$. This is because the microscopic reinforcing and toughening effects of $CaCO_3$ whiskers improves the matrix properties and then enhances the pullout behavior of steel fibers and PVA fibers (Cao et al., 2015; Pan et al., 2018). Therefore, a higher residual bearing capacity for post-peak stage can be achieved, i.e., a more noticeable softening stage for tensile stress-strain curves.

TABLE 4 Interfacial bonding strength of steel fiber and PVA fiber.

Fiber type	0% whisker	1% whisker	2% whisker	Reference
Hooked steel fiber	7.0	7.2	7.5	Wu and Li. (1999), Voo and Foster. (2003)
PVA fiber	1.37	1.45	1.85	Ma et al. (2017)

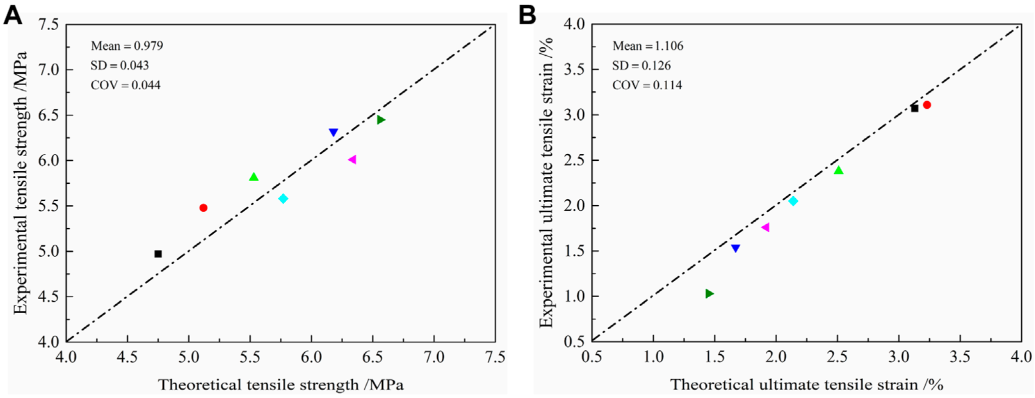

FIGURE 12
Calculation results of tensile strength and ultimate tensile strain.

The triple-line model needs to determine three key parameters, namely, stable cracking stress σ_{ss}, ultimate tensile stress σ_{cu} and ultimate tensile strain ε_{cu}, as illustrated in Figure 11. For the convenience of calculation, the first-peak stress σ_0 is numerically equal to the stable cracking stress σ_{ss} approximately, that is, the stress at the beginning of the strain hardening behavior. Therefore, the relationship of tensile stress $\sigma(\varepsilon)$ and tensile strain ε for MsHySHCCs can be expressed as Eq. 1.

$$\sigma(\varepsilon) = \begin{cases} E_c\varepsilon \; 0 \le \varepsilon < \frac{\sigma_{ss}}{E_c} \\ \sigma_{ss} + k_1\left(\varepsilon - \frac{\sigma_{ss}}{E_c}\right) \; \frac{\sigma_{ss}}{E_c} \le \varepsilon < \varepsilon_{cu} \\ k_2\sigma_{cu} \; \varepsilon_{cu} \le \varepsilon \end{cases} \quad (1)$$

Where k_1 is the hardening coefficient, $k_1 = \frac{\sigma_{cu}-\sigma_{ss}}{\varepsilon_{cu}-\sigma_{ss}/E_c}$; E_c is the elastic modulus of designed MsHySHCCs, which can be empirically obtained by fitting experimental data in this study and $E_c = -10.3RI_v^2 + 27.8RI_v + 1.8$; k_2 is the softening coefficient, $k_2 = \left(\frac{\varepsilon_{cu}}{\varepsilon}\right)^{\frac{4}{RI_v^2}}$; RI_v is the fiber reinforcing parameter (Ou et al., 2011; Ning et al., 2015), and RI_v can be obtained by Eq. 2.

$$RI_v = \sum_{i=1}^{n} \beta V_i \frac{l_i}{d_i}\left(\frac{E_i}{E_{sf}}\right)^p \quad (2)$$

The interfacial bonding parameter β can be considered as 1.0 for PVA fiber and 1.2 for steel fiber with hooked shape. Additionally, a stiffness factor p can be set as 1.3 for PVA fiber. The fiber volume fraction, fiber geometric length, and diameter are denoted as V_i, l_i, and d_i, respectively. Furthermore, E_i represents the fiber elastic modulus, while E_{sf} signifies the elastic modulus of hooked steel fiber.

The ultimate tensile stress σ_{tu} can be calculated by using the equation provided by Li and Leung in 1992, as shown in Eq. 3. The first-peak stress σ_0 can be calculated by Eq. 4. The hardening coefficient g can be determined by Eq. 5. The interfacial bonding strength τ_i can be determined according to Table 4.

$$\sigma_{tu} = g\sigma_0 \quad (3)$$

$$\sigma_0 = \frac{V_{i,pva}\tau_{i,pva}}{2}\left(\frac{l_{i,pva}}{d_{i,pva}}\right) + \frac{V_{i,sf}\tau_{i,sf}}{2}\left(\frac{l_{i,sf}}{d_{i,sf}}\right) \times F_{be} \quad (4)$$

$$g = \frac{2}{4+f^2}\left(1 + e^{\pi f/2}\right) \quad (5)$$

The hooked steel fiber characteristic parameter F_{be} was set as 1.7. Additionally, the hardening effect was taken into consideration using the factor f (Ahmed et al., 2007). In this study, the f values assigned to the matrix with 0%, 1%, and 2% $CaCO_3$ whiskers were 0.085, 0.105, and 0.125 respectively.

To characterize the ductility of SHCC, it is necessary to theoretically calculate the ultimate tensile strain ε_{tu} (Lin and Li, 1997), as provided in Eq. 6.

$$\varepsilon_{tu} = \frac{\delta_{tu}}{x_d} \quad (6)$$

Based on earlier research (Li and Stang, 1997; Lin and Li, 1997; Kanda and Li, 2000), the ultimate crack opening displacement δ_{tu} can be calculated by Eq. 7.

$$\delta_{tu} = \frac{\tilde{l}_f}{2}\left(\frac{c-2}{3c}\right) \quad (7)$$

Where $c = \frac{\gamma \tilde{l}_f}{2\tilde{d}_f}$; γ is a dimensionless factor (Wang et al., 1988; Shao et al., 1993), set as 0.5 in this study (Wu and Li, 1999). The

10.3389/fmats.2024.1378089

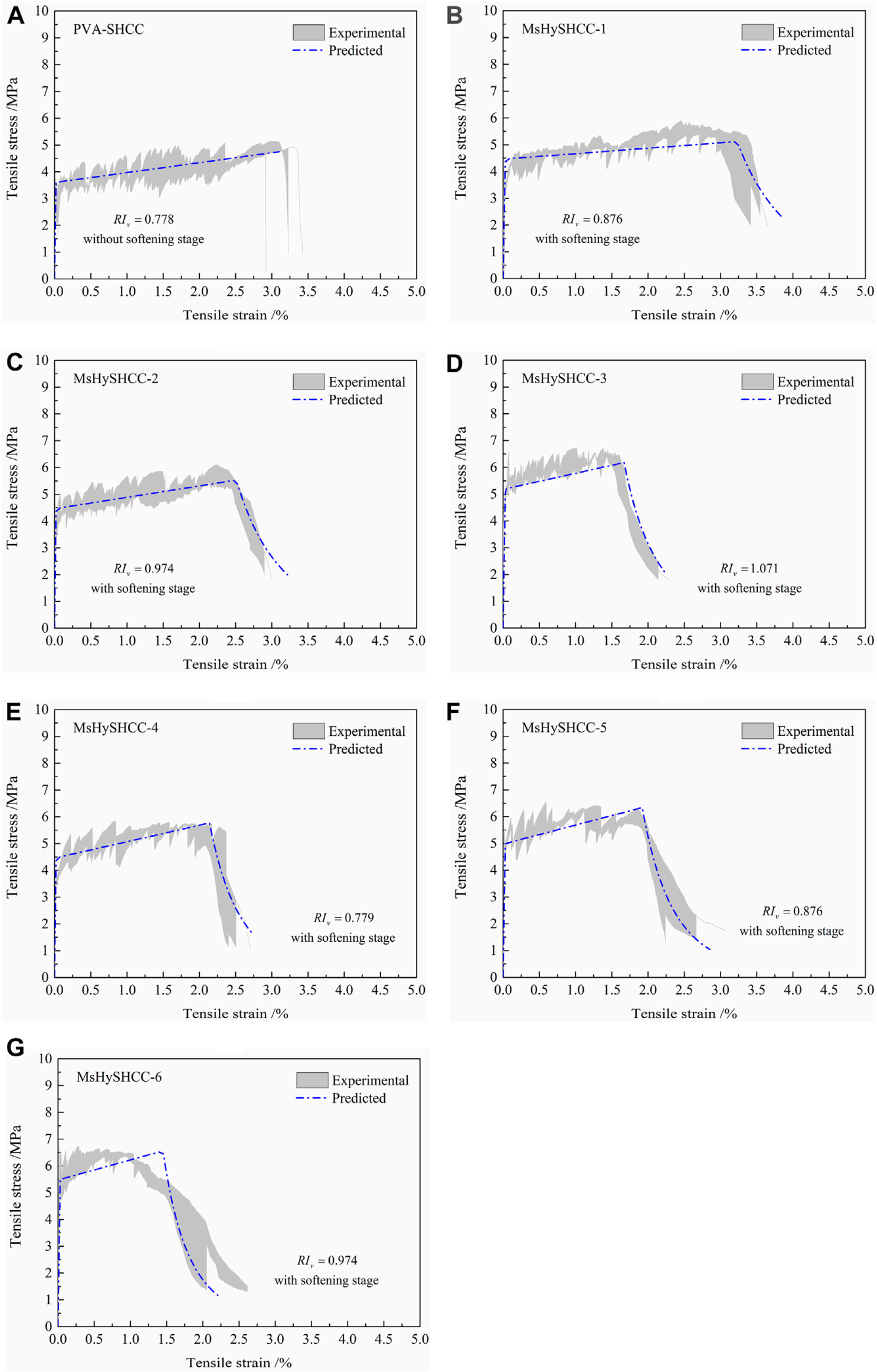

FIGURE 13
Calculation results of tensile constitutive relationship curves.

parameter $\tilde{l}_f$ and $\tilde{d}_f$ signifies the generalized mean value of fiber length and fiber diameter, respectively.

According to previous literature (Wu and Li, 1992; Alwan, 1994; Kanda and Li, 1998; Wu and Li, 1995), the crack spacing value x_d can be determined by Eq. 8.

$$x_d = \frac{\tilde{l}_f - \sqrt{\tilde{l}_f^2 - 2\pi\psi\tilde{l}_f x}}{2 - 2F(\tilde{c}_{mc})} \tag{8}$$

Where $\psi = \frac{4}{\pi g}$, $x = \frac{V_m \sigma_{mu} \tilde{d}_f}{4 V_f \tilde{\tau}_f}$, $F(\bar{c}_{mc}) = \exp\left[-\frac{1}{\lambda}\left(\frac{\bar{c}_0}{\bar{c}_{mc}}\right)^m\right]$ and $\bar{c}_0 = \left(\frac{\sqrt{\pi}}{2}\frac{K_m}{\sigma_{mu}}\right)^2$. The tensile strength of mortar σ_{mu} for 0%, 1% and 2% whiskers is taken as 3.0, 3.5, and 3.75 MPa, respectively; V_m is the volume fraction of mortar; the Weibull parameter m is taken as 2 and the normalized flaw size is set as 10 μm (Wu and Li, 1992); the fracture toughness of mortar is set as 0.37 MPa·m$^{1/2}$ (Ahmed et al., 2007).

Figures 12, 13 showcase the theoretical findings related to the tensile parameters and stress-strain curves. It can be seen that the proposed model adequately characterizes the tensile stress-strain correlation of MsHySHCC. Nevertheless, to a certain degree, the proposed model overestimates the cracking saturation degree of MsHySHCC and traditional PVA-SHCC during the experiment. Consequently, the calculated ultimate tensile strain values surpass the corresponding experimental measurements.

4 Conclusion

The aim of this study was to examine the tensile characteristics of SHCC reinforced with hybrid fibers at multiple scales (MsHySHCC). Two main questions were responded in this study. The initial step involves achieving a kind of MsHySHCC with both high strength and ductility. The second one is how to predict the tensile behaviors of MsHySHCC. This study yields the subsequent fundamental findings.

(1) PVA fibers control the tensile ductility of MsHySHCC. Steel fibers have a more pronounced effect on the tensile strength, but do not improve the tensile ductility of MsHySHCC. The tensile strength and tensile deformation capacity of the SHCC matrix can be significantly enhanced due to the micro-mechanisms involving $CaCO_3$ whiskers. The improved effect of whiskers on the mechanical properties of the matrix can further strengthen the pull-out mechanism of PVA fibers and steel fibers.

(2) Designing MsHySHCC is one of the effective ways to simultaneously enhance the strength and ductility of PVA-SHCC. The designed MsHySHCC shows higher tensile strength than that of traditional PVA-SHCC. Replacing some of the PVA fibers with $CaCO_3$ whiskers and hooked steel fibers at a volume fraction of 0.25% can result in increased tensile strength and ultimate tensile strain. However, a substantial decrease in the PVA fiber amount will greatly diminish the tensile ductility.

(3) By considering the impact of hybrid fibers and $CaCO_3$ whiskers, a semi-theoretical model was developed to describe the tensile constitutive relationship of the designed MsHySHCC. The comparison between the theoretical and experimental findings leads to the conclusion that this semi-theoretical model is capable of determining the tensile stress-strain relationships of MsHySHCC.

Data availability statement

The original contributions presented in the study are included in the article/Supplementary material, further inquiries can be directed to the corresponding author.

Author contributions

JH: Investigation, Writing–original draft, Writing–review and editing. JB: Investigation, Writing–review and editing. HM: Investigation, Writing–review and editing. ZX: Investigation, Writing–review and editing.

Funding

The author(s) declare that no financial support was received for the research, authorship, and/or publication of this article.

Conflict of interest

Authors JH, JB, HM, and ZX were employed by Zhenjiang Port Group Co., Ltd.

Publisher's note

All claims expressed in this article are solely those of the authors and do not necessarily represent those of their affiliated organizations, or those of the publisher, the editors and the reviewers. Any product that may be evaluated in this article, or claim that may be made by its manufacturer, is not guaranteed or endorsed by the publisher.

References

Ahmed, S. F., Maalej, M., and Paramasivam, P. (2007). Analytical model for tensile strain hardening and multiple cracking behavior of hybrid fiber-engineered cementitious composites. *J. Mater. Civ. Eng.* 19 (7), 527–539. doi:10.1061/(asce)0899-1561(2007)19:7(527)

Alwan, J. M. (1994). *Modeling of the mechanical behavior of fiber reinforced cement based composites under tensile loads*. PH.D. Dissertation. Michigan: University of Michigan.

Andreasen, A., and Andersen, J. (1930). About the relationship between grain and gradation gap in products of loose grains (with a few experiments). *Kolloid-Zeitschrift* 50 (3), 217–228. doi:10.1007/bf01422986

Arain, M. F., Memon, H., Wang, M., Ahmed, A., Chen, J., and Zhang, H. (2023). Matrix tailoring for polyvinyl alcohol (PVA) fiber-reinforced ductile cementitious composites. *AATCC J. Res.* 10 (2), 63–72. doi:10.1177/24723444221147982

ASTM (2010). *Standard test method for flexural performance of fiber-reinforced concrete (using beam with third-point loading)*. C1609/C1609M. West Conshohoken, PA: ASTM.

Betterman, L., Ouyang, C., and Shah, S. (1995). Fiber-matrix interaction in microfiber reinforced mortar. *Adv. Cem. Based Mater.* 2, 53–61. doi:10.1016/1065-7355(94)00027-b

Cao, M., Xie, C., Li, L., and Khan, M. (2019). Effect of different PVA and steel fiber length and content on mechanical properties of $CaCO_3$ whisker reinforced cementitious composites. *Mater. Construcc.* 69 (336), 200. doi:10.3989/mc.2019.12918

Cao, M., Zhang, C., Li, Y., and Wei, J. (2015). Using calcium carbonate whisker in hybrid fiber-reinforced cementitious composites. *J. Mater. Civ. Eng.* 27 (4), 1–13. doi:10.1061/(asce)mt.1943-5533.0001041

Deshpande, A., Kumar, D., and Ranade, R. (2019). Influence of high temperatures on the residual mechanical properties of a hybrid fiber-reinforced strain-hardening cementitious composite. *Constr. Build. Mater.* 208 (30), 283–295. doi:10.1016/j.conbuildmat.2019.02.129

Ding, Y., Yu, J., Yu, K., and Xu, S. l. (2018). Basic mechanical properties of ultra-high ductility cementitious composites: from 40 MPa to 120 MPa. *Compo. Struct.* 185, 634–645. doi:10.1016/j.compstruct.2017.11.034

Feng, J. Q. (2019). *Tensile properties of new hybrid fiber reinforced cementitious composites (NHyFRCC)*. Ph.D. Dissertation. Dalian: Dalian University of Technology.

Funk, J., and Dinger, D. (1994). *Predictive process control of crowded particulate suspensions*. New York, NY, USA: Springer.

Hermes, P., Zhang, Y., Soe, K., and Bell, J. (2012). Material properties of a new hybrid-fiber engineered cementitious composite. *Adv. Mater. Res.* 450-451, 433–438. 10.4028/www.scientific.net/amr.450-451.433.

Huang, T., Zhang, Y. X., and Yang, C. H. (2016). Multiscale modelling of multiple-cracking tensile fracture behaviour of engineered cementitious composites. *Eng. Fract. Mech.* 160, 52–66. doi:10.1016/j.engfracmech.2016.04.006

Hunger, M. (2010). *An integral design concept for ecological self-compacting concrete*. Ph.D. Dissertation. Eindhoven: Eindhoven University of Technology.

Kabele, P. (2007). Multiscale framework for modeling of fracture in high performance fiber reinforced cementitious composites. *Eng. Fract. Mech.* 74, 194–209. doi:10.1016/j.engfracmech.2006.01.020

Kanda, T., and Li, V. C. (1998). Multiple cracking sequence and saturation in fiber reinforced cementitious composites. *Concr. Res. Tech.* 9 (2), 19–32. doi:10.3151/crt1990.9.2_19

Kanda, T., and Li, V. C. (2000). Tensile stress-strain modeling of pseudo-strain hardening cementitious composites. *J. Mater. Civ. Eng.* 12 (2), 147–156. doi:10.1061/(asce)0899-1561(2000)12:2(147)

Kang, J., and Bolander, J. E. (2016). Multiscale modeling of strain-hardening cementitious composites. *Mech. Res. Commun.* 78, 47–54. doi:10.1016/j.mechrescom.2015.08.004

Karim, R., Najimi, M., and Shafei, B. (2019). Assessment of transport properties, volume stability, and frost resistance of non-proprietary ultra-high performance concrete. *Constr. Build. Mater.* 227, 117031. doi:10.1016/j.conbuildmat.2019.117031

Khalil, A. A., Atta, A. M., Baraghith, A. T., Behiry, R. N., and Soliman, O. E. (2023). Shear strengthening of concrete deep beams using pre-fabricated strain-hardening cementitious composite plates. *Eng. Struct.* 278, 115548. doi:10.1016/j.engstruct.2022.115548

Koichi, M., Tetsuya, I., and Toshiharu, K. (2003). Multi-scale modeling of concrete performance. *J. Adv. Concr. Technol.* 1, 91–126.

Li, V. C., and Leung, C. K. Y. (1992). Steady-state and multiple cracking of short random fiber composites. *J. Eng. Mech.* 11 (118), 2246–2264. doi:10.1061/(asce)0733-9399(1992)118:11(2246)

Li, V. C., and Stang, H. (1997). Interface property characterization and strengthening mechanisms in fiber reinforced cement based composites. *Adv. Cem. Based Mater.* 6 (1), 1–20. doi:10.1016/s1065-7355(97)90001-8

Lin, Z., and Li, V. C. (1997). Crack bridging in fiber reinforced cementitious composites with slip-hardening interfaces. *J. Mech. Phys. Solids* 45 (5), 763–787. doi:10.1016/s0022-5096(96)00095-6

Liu, J. C., and Tan, K. H. (2017a). Fire resistance of strain hardening cementitious composite with hybrid PVA and steel fibers. *Constr. Build. Mater.* 135, 600–611. doi:10.1016/j.conbuildmat.2016.12.204

Liu, J. C., Tan, K. H., and Fan, S. (2018). Residual mechanical properties and spalling resistance of strain-hardening cementitious composite with Class C fly ash. *Constr. Build. Mater.* 181 (30), 253–265. doi:10.1016/j.conbuildmat.2018.06.009

Liu, J. C., Tan, K. H., and Zhang, D. (2017b). Multi-response optimization of post-fire performance of strain hardening cementitious composite. *Cem. Concr. Compos.* 80, 80–90. doi:10.1016/j.cemconcomp.2017.03.001

Liu, T., Yang, Y., Chen, Z., Li, Y., and Bai, R. (2020). Optimization of fiber volume fraction to enhance reinforcing efficiency in hybrid fiber reinforced strain hardening cementitious composite. *Cem. Concr. Compos.* 113, 103704. doi:10.1016/j.cemconcomp.2020.103704

Ma, H., Cai, J., Lin, Z., Qian, S., and Li, V. C. (2017). $CaCO_3$ whisker modified engineered cementitious composite with local ingredients. *Constr. Build. Mater.* 151, 1–8. doi:10.1016/j.conbuildmat.2017.06.057

Maalej, M., Quek, S. T., Ahmed, S. F. U., Zhang, J., Lin, V., and Leong, K. (2012). Review of potential structural applications of hybrid fiber engineered cementitious composites. *Constr. Build. Mater.* 36, 216–227. doi:10.1016/j.conbuildmat.2012.04.010

Ning, X., Ding, Y., and Zhang, F. (2015). Experimental study and prediction model for flexural behavior of reinforced SCC beam containing steel fibers. *Constr. Build. Mater.* 93 (0), 644–653. doi:10.1016/j.conbuildmat.2015.06.024

Ou, Y., Tsai, M., Liu, K., and Chang, K. C. (2011). Compressive behavior of steel-fiber-reinforced concrete with a high reinforcing index. *J. Mater. Civ. Eng.* 24 (2), 207–215. doi:10.1061/(asce)mt.1943-5533.0000372

Pan, J., Cai, J., Ma, H., and Leung, C. K. Y. (2018). Development of multiscale fiber-reinforced engineered cementitious composites with PVA fiber and $CaCO_3$ whisker. *J. Mater. Civ. Eng.* 30 (6), 04018106. doi:10.1061/(asce)mt.1943-5533.0002305

Pan, Z., Wu, C., Liu, J., and Wang, W. (2015). Study on mechanical properties of cost-effective polyvinyl alcohol engineered cementitious composites (PVA-ECC). *Constr. Build. Mater.* 78, 397–404. doi:10.1016/j.conbuildmat.2014.12.071

Parant, E., Rossi, P., and Boulay, C. (2007a). Fatigue behavior of a multi-scale cement composite. *Cem. Concr. Res.* 37, 264–269. doi:10.1016/j.cemconres.2006.04.006

Parant, E., Rossi, P., and Maou, F. L. (2007b). Durability of a multiscale fibre reinforced cement composite in aggressive environment under service load. *Cem. Concr. Res.* 37, 1106–1114. doi:10.1016/j.cemconres.2006.02.021

Pierre, R., and Edouard, P. (2008). Damage mechanisms analysis of a multi-scale fibre reinforced cement-based composite subjected to impact and fatigue loading conditions. *Cem. Concr. Res.* 38, 413–421. doi:10.1016/j.cemconres.2007.09.002

Pourfalah, S. (2018). Behaviour of engineered cementitious composites and hybrid engineered cementitious composites at high temperatures. *Constr. Build. Mater.* 158, 921–937. doi:10.1016/j.conbuildmat.2017.10.077

Qasim, M., Lee, C. K., and Zhang, Y. X. (2023). Flexural strengthening of reinforced concrete beams using hybrid fibre reinforced engineered cementitious composite. *Eng. Struct.* 284, 115992. doi:10.1016/j.engstruct.2023.115992

Ramasamy, K. A., and Shanmughasundaram, K. (2018). Flexural performance of hybrid engineered cementitious composite layered reinforced concrete beams. *Period. Polytech. – Civ.* 62 (4), 921–929. doi:10.3311/ppci.11748

Rawat, S., Zhang, Y. C., and Lee, C. K. (2022). Multi-response optimization of hybrid fibre engineered cementitious composite using Grey-Taguchi method and utility concept. *Constr. Build. Mater.* 319, 126040. doi:10.1016/j.conbuildmat.2021.126040

Rossi, P., and Parant, E. (2008). Damage mechanisms analysis of a multi-scale fibre reinforced cement-based composite subjected to impact and fatigue loading conditions. *Cem. Concr. Res.* 38, 413–421. doi:10.1016/j.cemconres.2007.09.002

Shao, Y., Li, Z., and Shah, S. P. (1993). Matrix cracking and interface debonding in fiber-reinforced cement-matrix composites. *Adv. Cem. Based Mater.* 1 (2), 55–66. doi:10.1016/1065-7355(93)90010-l

Soe, K., Zhang, Y., and Zhang, L. (2013). Material properties of a new hybrid fibre-reinforced engineered cementitious composite. *Constr. Build. Mater.* 43, 399–407. doi:10.1016/j.conbuildmat.2013.02.021

Tinoco, M. P., and Silva, F. D. A. (2021). On the mechanical behavior of hybrid fiber reinforced strain hardening cementitious composites subjected to monotonic and cyclic loading. *J. Mater. Res. Tech.* 11, 754–768. doi:10.1016/j.jmrt.2021.01.053

Tran, N. T., Nguyen, T. K., Nguyen, D., and Le, Q. H. (2023). Assessment of fracture energy of strain-hardening fiber-reinforced cementitious composite using experiment and machine learning technique. *Struct. Concr.* 24 (3), 4185–4198. doi:10.1002/suco.202200332

Voo, J., and Foster, S. (2003). *Variable engagement model for fiber reinforced concretein tension UNICIV Report No. R-420*. Sydney: The University of New South Wales.

Wang, Y., Li, V. C., and Backer, S. (1988). Modelling of fibre pull-out from a cement matrix. *Int. J. Cem. Compos. Lightweight Concr.* 10 (3), 143–149. doi:10.1016/0262-5075(88)90002-4

Wang, Z., Zhang, J., and Wang, J. (2014). Tensile performance of polyvinyl alcohol–steel hybrid fiber reinforced cementitious composite with impact of water to binder ratio. *J. Compos. Mater.* 49 (18), 1–19. doi:10.1177/0021998314542450

Wu, H., and Li, V. C. (1992). Snubbing and bundling effects on multiple crack spacing of discontinuous random fiber-reinforced brittle matrix composites. *J. Am. Ceram. Soc.* 75 (12), 3487–3489. doi:10.1111/j.1151-2916.1992.tb04457.x

Wu, H., and Li, V. C. (1995). Stochastic process of multiple cracking in discontinuous random fiber reinforced brittle matrix composites. *Int. J. Damage Mech.* 4 (4), 83–102. doi:10.1177/105678959500400105

Wu, H., and Li, V. C. (1999). Fiber/cement interface tailoring with plasma treatment. *Cem. Concr. Compos.* 21 (3), 205–212. doi:10.1016/s0958-9465(98)00053-5

Xie, C., Cao, M., Si, W., and Khan, M. (2020). Experimental evaluation on fiber distribution characteristics and mechanical properties of calcium carbonate whisker modified hybrid fibers reinforced cementitious composites. *Constr. Build. Mater.* 265, 120292. doi:10.1016/j.conbuildmat.2020.120292

Zhang, C., and Cao, M. (2014). Fiber synergy in multi-scale fiber-reinforced cementitious composites. *J. Reinf. Plast. Comp.* 33 (9), 862–874. doi:10.1177/0731684413514785

Zhang, J., Wang, Q., and Wang, Z. (2016). Properties of polyvinyl alcohol-steel hybrid fiber reinforced composite with high-strength cement matrix. *J. Mater. Civ. Eng.* 29 (7), 1–9. doi:10.1061/(asce)mt.1943-5533.0001868

Zhang, Y., Deng, M., and Dong, Z. (2019). Seismic response and shear mechanism of engineered cementitious composite (ECC) short columns. *Eng. Struct.* 192, 296–304. doi:10.1016/j.engstruct.2019.05.019

Zhang, Z. G., Li, Z., He, J., and Shi, X. (2023b). High-strength engineered cementitious composites with nanosilica incorporated: mechanical performance and autogenous self-healing behavior. *Cem. Concr. Compos.* 135, 104837. doi:10.1016/j.cemconcomp.2022.104837

Zhang, Z. G., Liu, J., Li, J., Qin, F., and Di, J. (2023a). Micromechanics-based analysis of PVA-ECC after thermal exposure. *Arch. Civ. Mech. Eng.* 23, 213. doi:10.1007/s43452-023-00736-1

Zhang, Z. G., Liu, S., Yang, F., Weng, Y., and Qian, S. (2021). Sustainable high strength, high ductility engineered cementitious composites (ECC) with substitution of cement by rice husk ash. *J. Clean. Prod.* 317, 128379. doi:10.1016/j.jclepro.2021.128379

Zhang, Z. G., Qin, F., Ma, H., and Xu, L. (2020a). Tailoring an impact resistant engineered cementitious composite (ECC) by incorporation of crumb rubber. *Constr. Build. Mater.* 262, 120116. doi:10.1016/j.conbuildmat.2020.120116

Zhang, Z. G., Yang, F., Liu, J., and Wang, S. (2020b). Eco-friendly high strength, high ductility engineered cementitious composites (ECC) with substitution of fly ash by rice husk ash. *Cem. Concr. Res.* 137, 106200. doi:10.1016/j.cemconres.2020.106200

Zhao, X., Li, Q., and Xu, S. (2020). Contribution of steel fiber on the dynamic tensile properties of hybrid fiber ultra-high toughness cementitious composites using Brazilian test. *Constr. Build. Mater.* 246, 118416. doi:10.1016/j.conbuildmat.2020.118416

Zhou, J., Pan, J., and Leung, C. (2015). Mechanical behavior of fiber reinforced engineered cementitious composites in uniaxial compression. *J. Mater. Civ. Eng.* 27 (1), 04014111. doi:10.1061/(asce)mt.1943-5533.0001034